

Inverse Problems of Aggregation Processes

H. Wright,¹ R. Muralidhar,¹ T. Tobin,¹ and D. Ramkrishna^{1,2}

Received April 21, 1989; final February 27, 1990

The coagulation frequency is the key ingredient in the population balance (Smoluchowski) equation of coagulation kinetics. An inverse problem is formulated to extract the coagulation frequency from transient size distributions when these distributions are self-similar. Two numerical examples illustrate the procedure. The first demonstrates the inverse problem for the recovery of singular coagulation frequencies, while the second shows the procedure when self-similarity is approximate. Transient droplet coagulation experiments in a turbulent flow field have been performed. The resulting size distributions are observed to be self-similar. The inverse problem is used to determine the drop coagulation frequency. This frequency shows significant deviation from the coagulation frequencies derived from simple models of drop-drop interactions in a turbulent flow field.

KEY WORDS: Inverse problem; agglomeration kinetics; scaling spectra; coagulation frequency.

1. INTRODUCTION

Aggregation is the process by which distinct particles or droplets combine physically to form a single unit. The kinetics of irreversible aggregation processes are described in the *mean field approach* by the well-known coagulation equation due to Smoluchowski,⁽¹⁾

$$\begin{aligned} \frac{\partial n(v, t)}{\partial t} = & \frac{1}{2} \int_0^v q(v-v', v', \dots) n(v-v', t) n(v', t) dv' \\ & - \int_0^\infty q(v, v', \dots) n(v, t) n(v', t) dv' \end{aligned} \quad (1.1)$$

¹ School of Chemical Engineering, Purdue University, West Lafayette, Indiana 47907.

² To whom correspondence should be addressed.

In the above, $n(v, t)$ is the number density of particles of volume v at time t and $q(v, v', \dots)$ is the coagulation frequency of particles of volumes v and v' , which also depends on other physical parameters represented by the dots. Given the coagulation frequency function, the agglomeration equation can be employed to predict the evolution of size spectra from any initial distribution $n(v, 0)$. The coagulation equation has been a basis for understanding the formation of smoke and haze,⁽²⁾ growth of polymer chains in solution,⁽³⁾ fractal growth of proteins,⁽⁴⁾ gelation phenomena,⁽⁵⁾ etc.

The key ingredient of the mean field approach to coagulation is the coagulation frequency function $q(v, v', \dots)$, which depends on the nature of the relative motion of particle pairs in the suspending medium. The coagulation frequency $q(v, v', \dots)$ also depends on many physical parameters of the system, such as the interfacial tension, turbulence energy dissipation in a turbulent flow field, the viscosities of both phases, etc. The frequency may even be a functional of the transient size distributions, especially at higher particle fractions.

The agglomeration frequency is usually derived from mechanistic models of the relative motion between a pair of particles. A classic example is the coagulation frequency of Brownian particles due to Smoluchowski.⁽¹⁾ Smoluchowski's model determines the agglomeration frequency by describing the relative motion as diffusion. The agglomeration coefficients of polymers are presented by Ernst.⁽³⁾ Such models and frequencies are then evaluated based on their ability to describe experimental coagulation data.

The coagulation frequency function has been hitherto regarded as an entity which can be only derived by methods outside the Smoluchowski equation framework. Extracting the coagulation frequency from transient size distributions can be termed an inverse problem. While the direct problem of coagulation kinetics is concerned with the prediction of transient cluster size distributions using known agglomeration frequency functions, the inverse problem of aggregation is aimed at recovering the coagulation frequency function from transient size spectra in situations where the frequencies are unknown. The inverse problem formulation is particularly useful in situations where reciprocal effects between the motion of the particles and the suspending medium or many-body effects make the formulation of models of the relative motion difficult. In fact, the frequencies obtained from the inverse problem may be used to identify the salient dynamical features influencing coagulation.

The direct determination of the coagulation frequency from raw transient experimental data by inverting the Smoluchowski equation is extremely difficult. However, numerical experiments,⁽⁶⁾ theoretical analysis of the asymptotic properties of size spectra of different coagulation

kernels,⁽⁷⁾ as well as empirical evidence⁽⁸⁾ suggest that at large coagulation times the size spectra may be self-similar. The scaling spectrum is defined by⁽²⁾

$$\Psi(z) = n(v, t) \bar{v}^2(t), \quad z = v/\bar{v}(t)$$

where $\bar{v}(t)$ is the average size of the population at time t . Basically, the transient number densities at large times can be expressed by a single function $\Psi(z)$ (similarity distribution) of a scaled size variable z . The inverse problem then becomes one of identifying the coagulation frequency function from the self-similar distribution. Muralidhar and Ramkrishna⁽⁹⁾ formulated an inverse problem to derive homogeneous coagulation frequencies from similarity spectra and subsequently⁽¹⁰⁾ generalized it to accommodate certain nonautonomous, nonhomogeneous kernels which also exhibit scaling spectra.

The objectives of this paper are threefold. First, the earlier formulation of the inverse problem is simplified and made more general. Methods to diagnose and extract singular frequency functions (for example, Brownian coagulation frequency) are presented and illustrated with an example. Second, the applicability of the inverse problem to situations of approximate scaling behavior is investigated. In this context, the concept of approximate similarity and frequencies that can display approximate similarity are discussed. Finally, the formulation is used to determine the coagulation frequency from experimental scaling size spectra of coalescing droplets in a turbulent flow field. This is a situation where the modeling of the coagulation frequency based on relative motion is complicated by hydrodynamic interactions as well as Coulombic interactions between the droplets at small separations. The outline of this paper is as follows: In Section 2, similarity, approximate similarity, and the inverse problem formulation are presented. Section 3 describes briefly the numerical algorithms. In Section 4 numerical examples for nonhomogeneous and singular agglomeration kernels are described. In Section 5 the inverse problem is used to determine the coagulation frequency from experimental size distributions of droplets in a turbulent flow field. The salient aspects are summarized in Section 6.

2. SIMILARITY SPECTRA AND THE INVERSE PROBLEM

The Smoluchowski equation, Eq. (1.1), written in terms of the cumulative volume fraction is

$$\frac{\partial F(v, t)}{\partial t} = - \int_0^v dF(v', t) \int_{v-v'}^{\infty} \frac{dF(v'', t)}{v''} q(v', v'', \dots) \quad (2.1)$$

where the cumulative volume fraction $F(v, t)$ is

$$F(v, t) = \int_0^v v'n(v', t) dv' \tag{2.2}$$

The following scaling transformation⁽²⁾ is introduced:

$$F(v, t) \rightarrow f(z), \quad z = vs(t) \tag{2.3}$$

where $s(t)$ is the inverse of the mean particulate size at time t . Frequently employed choices for $s(t)$ are

$$(a) \quad s(t) = \frac{M_0(t)}{M_1(t)}, \quad (b) \quad s(t) = \frac{M_1(t)}{M_2(t)}, \quad (c) \quad s(t) = \frac{M_2(t)}{M_3(t)} \tag{2.4}$$

In the above, $M_p(t)$ is the p th moment of the distribution at time t and is given by

$$M_p(t) = \int_0^\infty v^p n(v, t) dv, \quad p = 0, 1, \dots, \quad M_1(t) \equiv 1$$

Not all the above choices for $s(t)$ may yield a similarity distribution.⁽³⁾ For example, the well-studied sum coagulation kernel $v + v'$ does not yield similarity with respect to Eq. (2.4a). Of course, choices more general than the above are possible, but will not be of interest here. Under the similarity transformation (2.3), Eq. (2.1) yields

$$zf'(z) = -\frac{s^2}{s'(t)} \int_0^z df(z') \int_{z-z'}^\infty \frac{df(z'')}{z''} q\left(\frac{z'}{s}, \frac{z''}{s}, \dots\right) \tag{2.5}$$

where the primes on s and f denote the derivatives of these functions with respect to their arguments.

Further simplification is possible upon analyzing the consequences of the similarity criterion. Under conditions where similarity spectra are observed, Eq. (2.5) requires that

$$\frac{\partial}{\partial t} \left(\frac{s^2}{s'(t)} \int_0^z df(z') \int_{z-z'}^\infty \frac{df(z'')}{z''} q\left(\frac{z'}{s}, \frac{z''}{s}, \dots\right) \right) = 0 \tag{2.6}$$

The above is the most general criterion for similarity behavior. In what follows, we restrict ourselves to situations where the density function $f'(z)$ has at most an order of singularity one at the origin. This leads to the conclusion that

$$q\left(\frac{z'}{s(t)}, \frac{z''}{s(t)}, \dots\right) = S(s(t)) b(z', z'') \tag{2.7}$$

where $S(s(t))$ is some function of the reciprocal mean volume at time t and the dependence of $b(z', z'')$ on other physical parameters is understood. Substituting Eq. (2.7) into Eq. (2.5) and requiring similarity yields

$$s'(t) s^2(t) S^{-1}(t) = -a_m \tag{2.8}$$

and

$$a_m z f'(z) = \int_0^z \int_{z-z'}^\infty f'(z) \frac{f'(z'')}{z''} b(z', z'') dz'' dz' \tag{2.9}$$

where a_m is the separation constant.

As an illustration, we consider an important class of coagulation kernels that are studied in the literature which are homogeneous functions of the cluster sizes. These have the property that

$$q(\lambda v, \lambda v') = \lambda^m q(v, v'), \quad \lambda > 0 \tag{2.10}$$

where m is the degree of homogeneity. These frequencies satisfy Eq. (2.7) with $S = s^{-m}$ and $b(z', z'') = q(z', z'')$. According to Eq. (2.7), nonhomogeneous agglomeration frequencies can yield scaling spectra only if they show explicit dependence on the mean agglomerate size. An example in this category is the frequency derived by Wang,⁽¹²⁾

$$q(v, v') = c' \frac{e^{-a'(v+v')} + e^{-b'(v+v')}}{(e^{-a'v}/a' + e^{-b'v}/b')(e^{-a'v'}/a' + e^{-b'v'}/b')} \tag{2.11}$$

where

$$a' = as(t), \quad b' = bs(t), \quad c' = \frac{c}{s(t)^2}$$

In this case $S = 1$ and $b(z', z'')$ is given by the function (2.11) with constant parameters $a, b,$ and c replacing the corresponding primed parameters.

Many frequencies may not be homogeneous, with the nonhomogeneity arising primarily due to a mass-dependent sticking or reaction probability which depends on the details of the collision cross section. Such frequencies may display self-similar behavior in an approximate sense. We make the following transformation first suggested by Wang and Friedlander⁽¹³⁾:

$$F(v, t) \rightarrow f(z, t), \quad z = vs(t) \tag{2.12}$$

and letting

$$\left\| \frac{s(t)}{s'(t)} \frac{\partial}{\partial t} f(z, t) \right\| \ll \left\| z \frac{\partial}{\partial z} f(z, t) \right\| \tag{2.13}$$

for an interval of time then *approximate similarity* is attained and Eqs. (2.7)–(2.9) hold in an approximate sense on the time interval.

Identification of the function $S(s(t))$ is possible by exploiting properties of certain classes of coagulation frequencies. We consider a broad class of agglomeration frequencies whose scaling spectra may be self-similar or approximately self-similar. Most coagulation frequencies known in the literature possess the property

$$q\left(\frac{z'}{s(t)}, \frac{z''}{s(t)}, \dots\right) = s(t)^{-m} h(z', z'')[A + p(z', z'', s)] \quad (2.14)$$

where $h(z', z'')$ is a homogeneous function of degree m and $p(z', z'', s)$ is in general nonhomogeneous. If $p(z', z'', s)$ is not a function of $s(t)$, then the agglomeration frequency is a candidate for generating self-similar size distributions and if $p(z', z'', s) \simeq \bar{p}(z', z'')$ as $s \rightarrow 0$, then it is a candidate for approximate similarity. Upon substituting this form for the agglomeration kernel into Eq. (2.5), we find that

$$S(s(t)) = s(t)^{-m}$$

and Eq. (2.8) yields

$$s'(t) s(t)^{m-2} = -a_m \quad (2.15)$$

This equation may be integrated to obtain

$$\begin{aligned} s(t)^{m-1} &= A + a_m(1-m)t, & m \neq 1 \\ s(t) &= A \exp(-a_1 t), & m = 1 \end{aligned} \quad (2.16)$$

where a_m is a separation constant for the interval over which scaling or approximate scaling of size spectra is observed. In what follows we will restrict ourselves to cases where $S(s(t)) = s(t)^{-m}$.

We cast the above in more meaningful terms by considering a typical example. The coagulation frequency of Brownian particles when slip is important is given by⁽¹³⁾

$$q(v, v') = (v^{1/3} + v'^{1/3})[v^{-1/3} + v'^{-1/3} + \gamma(v^{-2/3} + v'^{-2/3})] \quad (2.17)$$

where γ is a constant. This nonhomogeneous frequency function can be cast in the form given by Eq. (2.14) with the identification of

$$\begin{aligned} A &= 1, & h(z, z') &= (z^{1/3} + z'^{1/3})(z^{-1/3} + z'^{-1/3}) \\ p(z', z'', s) &= \gamma s^{1/3}(z^{-2/3} + z'^{2/3})(z^{-1/3} + z'^{-1/3})^{-1} \end{aligned}$$

As s tends to zero, $p(z', z'', s)$ tends to zero also. In other words, the scaling frequency behaves like a homogeneous one for vanishing values of s . In this case we have a sequence of self-preserving spectra at large times converging asymptotically to the spectrum of the Brownian frequency.⁽¹³⁾

Experimentally observed self-similar behavior will often be approximate due to two reasons. First, even in cases where scaling behavior is possible, such spectra are only attained asymptotically at large times. Second, even homogeneous coagulation kernels can often have non-homogeneous second-order correction terms which do not admit a similarity transformation of the coagulation equation.

The coagulation frequency is determined from the knowledge of the parameter m and the function $b(z', z'')$. The identification proceeds in two stages. First, the parameters m and a_m are identified from a fit of $s(t)$ data to Eq. (2.16). Subsequently, $b(z', z'')$ is obtained from Eq. (2.9).

3. COMPUTATIONAL STRATEGIES

The inverse problem given by Eq. (2.9) is difficult to solve due to two reasons. First of all, it is an integral equation of the first kind and is consequently an ill-posed problem.⁽¹⁴⁾ By this is meant that small uncertainties in the data $f'(z)$ can introduce large errors in the solution $b(z', z'')$. Second, the unknown function is a function of two variables and hence a large number of expansion coefficients may be required. The first difficulty is overcome by the technique of Tikhonov regularization of ill-posed problems.⁽¹⁴⁾ The latter difficulty may be overcome by choosing an appropriate basis set of expansion.⁽¹⁵⁾

The technique of regularization is made transparent by casting Eq. (2.9) in operator notation. On defining

$$g(z) = a_m z f'(z), \quad k(z', z'') = \frac{f'(z') f'(z'')}{z''} \tag{3.1}$$

Eq. (2.9) becomes

$$g(z) = \int_0^z dz' \int_{z-z'}^\infty dz'' k(z', z'') b(z', z'') \tag{3.2}$$

The above can be succinctly cast as

$$\mathbf{Kb} = \mathbf{g} \tag{3.3}$$

where \mathbf{b} and \mathbf{g} are vectors and \mathbf{K} is an integral operator described by Eq. (3.2). The idea of regularization is to replace the ill-posed problem by the well-posed approximation

$$\text{Minimize } \|\mathbf{Kb} - \mathbf{g}\|_1^2 + \lambda \|\mathbf{b}\|_2^2 \tag{3.4}$$

where the subscripts on $\|$ indicate different norms for the two vector spaces and λ is small, nonnegative regularization parameter. The first term in Eq. (3.4) measures the residual, whereas the second term is the norm of the solution with the regularizing parameter acting as the weighting factor. Basically this procedure filters off the high-frequency components of the solution which tend to be corrupted by experimental noise. As the noise in the data increases, the regularizing parameter must be increased to discard more frequency components of the solution. In the Tikhonov regularization procedure, the regularization parameter λ is chosen so as to be commensurate with the quality of the data. This is explained in more detail in Section 5.

In order to obtain an adequate finite-dimensional approximation of Eq. (3.4), an appropriate Hilbert space must be chosen to expand $b(z', z'')$. A computationally useful Hilbert space is $\{L_2(0, \infty) \times L_2(0, \infty); x^{2|\mu|}e^{-x}y^{2|\mu|}e^{-y}\}$, where $|\mu|$ is the order of singularity of the unknown function $b(z', z'')$. The Laguerre polynomials may be used to construct the basis set for expanding the solution. The Laguerre polynomials are defined by⁽¹⁶⁾

$$L_i(s) = e^s \frac{d(s^i e^{-s})}{ds^i}, \quad i = 0, 1, \dots$$

The basis is now readily obtained as the tensor product of the functions $\{\phi_i\}$ defined by

$$\phi_i(x) = x^{-|\mu|} L_i(x) \tag{3.5}$$

The unknown function is expressed as a linear combination

$$b(z', z'') = \sum_{i=0}^{n-1} \sum_{j=0}^{n-1} \alpha_{ij} \phi_i(z') \phi_j(z'') \tag{3.6}$$

where α_{ij} are the unknown coefficients to be determined. On letting

$$a_{ipq} = \int_0^{z_i} dz' \int_{z_i-z'}^{z_{\max}} dz'' f'(z') \frac{f'(z'')}{z''} \phi_p(z') \phi_q(z'') \tag{3.7}$$

and

$$g_i = z_i f'(z_i) a_m \tag{3.8}$$

the minimization problem given by Eq. (3.4) becomes

$$\text{Minimize } \sum_{i=1}^r \sum_{pq} (a_{ipq} \alpha_{pq} - g_i)^2 + \lambda \sum_{pq} \sum_{vs} \alpha_{pq} \alpha_{vs} h_{pq} h_{vs} \tag{3.9}$$

where r is the number of collocation points chosen on the interval $(0, z_{\max})$ and

$$h_{ij} = \int_0^{\infty} x^{2|\mu|} e^{-x} \phi_i(x) \phi_j(x) dx = \delta_{ij} \quad (3.10)$$

The symmetry of the agglomeration frequency implies that

$$\alpha_{pq} = \alpha_{qp} \quad (3.11)$$

A constrained minimization algorithm can be used to solve Eqs. (3.9) and (3.11).

It remains to identify the singularity of the unknown function $b(z', z'')$ from the similarity distribution. In this regard, one of the results of van Dongen and Ernst⁽¹¹⁾ can be used. They have shown that the order of singularity μ is related to the behavior of the similarity distribution $\Psi(z)$ near the origin. Whenever the coagulation frequency function is singular, particles of disparate sizes coagulate rapidly and the size spectrum Ψ tends to be peaked about the mean size. Van Dongen and Ernst⁽¹¹⁾ have shown that for singular homogeneous coagulation frequencies the leading behavior of similarity distribution near the origin is given by

$$\frac{f'(z)}{z} \simeq D \exp \left[- \frac{Kz^{-|\mu|}}{|\mu| a_m} \right] \quad \text{as } z \rightarrow 0 \quad (3.12)$$

where K and D can be considered constants to be determined when fitting $\Psi(z)$ for small values of z . While the form is strictly valid for homogeneous kernels, it is expected to be a good approximation if the nonhomogeneous corrections to the frequency are small.

4. NUMERICAL EXAMPLES

In this section, we present two numerical examples to illustrate the inverse problem procedure. The examples serve to test the applicability of the formulation under fairly severe conditions. The first situation considered is one where the coagulation frequency is singular. In the second example, we investigate the efficacy of the approach to realistic cases where the scaling behavior is only approximate. As mentioned earlier, strict dynamic scaling is an idealization and may be valid only when the short-range interactions between the particles negligibly influence the reaction cross section.

The numerical experiment is as follows. First, the discretized version of the coagulation equation⁽⁷⁾ is solved for a known agglomeration frequency

and the scaling spectrum is obtained. This scaling spectrum is now used to recover the frequency from the inverse problem. The closeness of the extracted function to the actual is measured by the relative error defined by

$$e_{\text{rel}} = \frac{\|q_{\text{actual}} - q_{\text{inverse}}\|}{\|q_{\text{actual}}\|}$$

where

$$\|f\| = \left(\int_0^2 \int_0^2 f^2(z', z'') dz' dz'' \right)^{1/2}$$

The limits of integration reflect the fact that almost all the particles have dimensionless size in this range.

4.1. Singular Agglomeration Frequencies

For many physical situations, it is known that the agglomeration frequency $q(v, v')$ is singular along the v and v' axes. For example, the Brownian coagulation frequency given by

$$q(v, v') = (v^{1/3} + v'^{1/3})(v^{-1/3} + v'^{-1/3}) \quad (4.1)$$

has such singularities along the v and v' axes. In such cases the similarity spectra $f'(z)/z$ vanish at the origin as discussed in Section 2. Physically, this is a consequence of the fact that particles of disparate sizes disappear quickly from the population. Experimental self-similar spectra can be used to identify the order of singularity via Eq. (3.12). For illustrative purposes, we consider the nonautonomous and nonhomogeneous frequency function

$$q(v, v') = (v^{1/3} + v'^{1/3})[v^{-1/3} + v'^{1/3} + \gamma s(t)^{-1/3} (v^{-2/3} + v'^{-2/3})] \quad (4.2)$$

This is the case of Brownian coagulation with slip where the mean free path is made time dependent. This frequency is a candidate for self-similar behavior, since $p(z, z', s) = p(z, z')$. The scaling spectrum for this frequency function obtained by numerical solution of a discretized version of Eq. (1.1) is shown in Fig. 1. The parameters m and a_m were determined by a least squares fit of Eq. (2.16). The value of m was determined to be 0.00. Since the similarity density $\Psi(z)$ approaches zero as z approaches zero, the unknown $b(z', z'')$ is singular along both axes. The degree of singularity $|\mu|$, determined by fitting the scaling spectrum near the origin to Eq. (3.12), is 0.658, in comparison to the actual value of $2/3$. The calculated degree of singularity is used to construct a set of orthogonal polynomials as outlined in Section 3. Three basis functions are used to expand the unknown

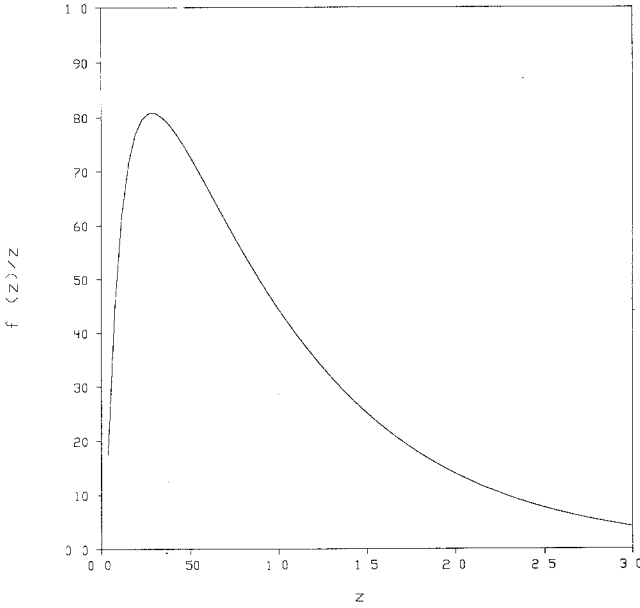


Fig. 1. Self-similar size spectrum for the agglomeration frequency given by Eq. (4.2).

function; therefore, only six unique coefficients are determined. Figure 2 compares the actual function with the function determined via the inverse problem. In this case the regularization parameter λ is set to be 0.1 and the relative error is 2.16%. The inverse problem result mimics the actual.

4.2. Approximate Similarity

We consider the coalescence frequency of droplets in a turbulent flow field⁽¹⁷⁾

$$q(v, v') = k(v^{1/3} + v'^{1/3})^{7/3} \eta_c \tag{4.3}$$

where

$$\eta_c = \frac{1 - \exp(-\phi\beta\xi^4)}{1 - \exp(-\beta\xi^4)} \tag{4.4}$$

In Eq. (4.4), ξ is the dimensionless harmonic mean radius of the pair of droplets, while ϕ ($0 < \phi < 1$) and β are parameters. Then

$$q\left(\frac{z'}{s(t)}, \frac{z''}{s(t)}, \dots\right) = s^{-7/9} (z^{1/3} + z'^{1/3})^{7/3} \frac{1 - \exp[-\phi\beta s^{-4/3} z^{4/3} z'^{4/3} / (z^{1/3} + z'^{1/3})^4]}{1 - \exp[-\beta s^{-4/3} z^{4/3} z'^{4/3} / (z^{1/3} + z'^{1/3})^4]}$$

Comparing this with the form given by Eq. (2.14), it is evident that $A = 0$, while the nonhomogeneous part is given by

$$p(z', z'', s) = \frac{1 - \exp[-\phi\beta s^{-4/3} z^{4/3} z'^{4/3} / (z^{1/3} + z'^{1/3})^4]}{1 - \exp[-\beta s^{-4/3} z^{4/3} z'^{4/3} / (z^{1/3} + z'^{1/3})^4]} \quad (4.5)$$

The nonhomogeneous part $p(z', z'', s)$ approaches unity as s becomes much smaller than unity and hence approximate scaling behavior is possible. The

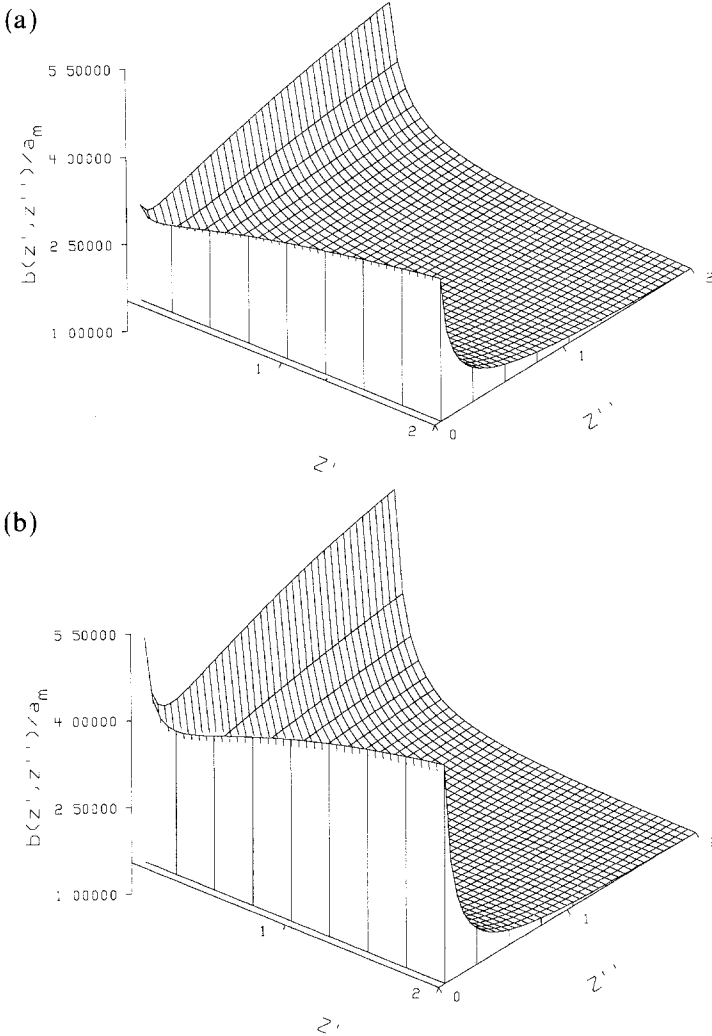


Fig. 2. The frequency function obtained from the inverse problem compared with the actual for Eq. (4.2). (a) Actual, (b) inverse problem result.

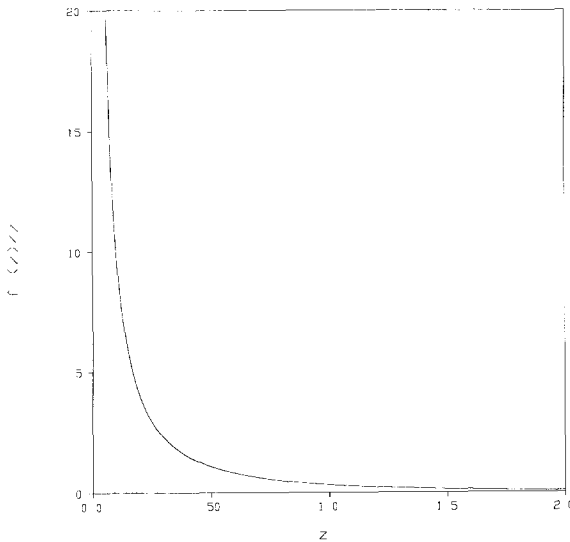


Fig. 3. Approximate scaling spectrum for the agglomeration frequency given by Eq. (4.3).

approximate scaling spectrum for small s is shown in Fig. 3. The values of m and a_m are again determined from a fit of the reciprocal scaling size $s(t)$ to Eq. (2.16). The parameter m is estimated to be 0.778, which is the actual value. With this spectrum, the inverse problem yields the frequency shown in Fig. 4. The actual function (over the same interval of s) is also displayed in the same figure. The regularizing parameter was set equal to 10^{-30} and the relative error is 4.65%. The extracted frequency function mimics the actual.

5. COAGULATION FREQUENCIES FROM EXPERIMENT

In this section experimental similarity distributions will be subjected to the inverse problem. As the actual frequency is unknown in this case, the veracity of the frequency obtained from the inverse problem can be established by testing its ability to predict the transient size distributions of the experiment. The physical system consists of neutrally buoyant organic phase droplets in a turbulent flow field. The coalescence frequency of droplets is difficult to derive from mechanistic models because the relative motion at small separations is influenced by hydrodynamic interaction and electrostatic and dispersion forces as well as droplet deformation. These difficulties make the inverse problem particularly useful.

The particular system chosen is a 5% dispersion of a neutrally buoyant mixture of benzene-carbon tetrachloride in water. The experiment

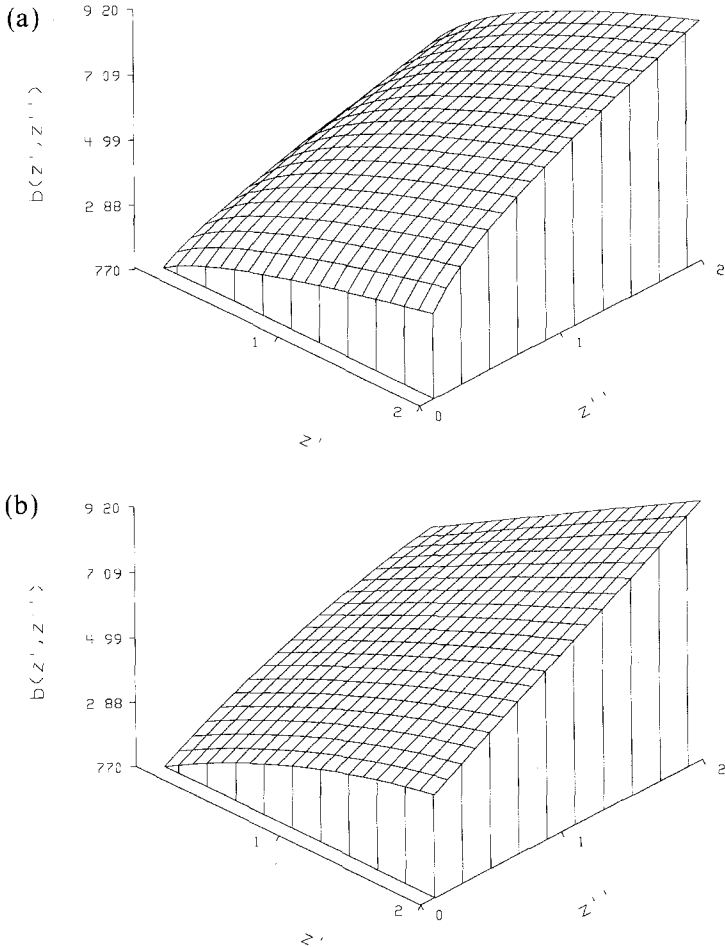


Fig. 4. The frequency function obtained from the inverse problem compared with the actual for Eq. (4.3). (a) Actual, (b) inverse problem result.

was conducted in a 2-liter stirred tank. A multitude of small drops was created at a high impeller stirring speed of 800 rpm. Coalescing transients were observed after a sudden reduction of the impeller speed to 200 rpm. Droplet fragmentation effects were negligible because the final turbulence intensity was insufficient to break the small drops. The size distribution was measured periodically by withdrawing small samples, immobilizing the drops with a surfactant, and photographing the samples. More experimental details are available elsewhere.⁽¹⁸⁾

Two experiments were performed sequentially. Initially the benzene-carbon tetrachloride was added to the water and was prestirred at 800 rpm for 1 hour. The impeller was then suddenly reduced to 200 rpm and a transient coalescence experiment was performed. After 3 hours, the impeller speed was again increased to 800 rpm for 1 hour. Another coalescence experiment was performed following a reduction of the impeller speed to 200 rpm. The initial conditions ($t=0$) for the two experiments are not identical because the histories of the two initial conditions were not identical. Therefore, the transient size distributions did not evolve identically. In spite of this, the transient size distributions of both experiments evolve to the same similarity spectrum quickly. The reciprocal mean size used is given by Eq. (2.4b). The functions $f'(z)$ and $f(z)$ are shown in Figs. 5 and 6. To facilitate solution of Eq. (2.9) for the function $b(z', z'')$, the density function $f'(z)$ is fit with a function

$$f'(z) = 0.3098z^{-0.0780} \exp(-0.7694z) + 11.0177z^{1.9086} \exp(-3.3840z) \tag{5.1}$$

This function satisfies the constraints $\int_0^\infty f'(z) dz = 1$ and $\int_0^\infty zf'(z) dz = 1$. The second constraint arises as a consequence of using the scaling volume

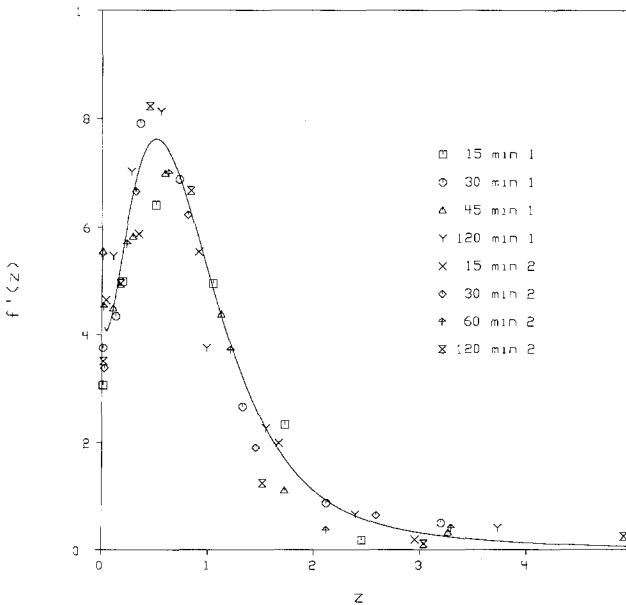


Fig. 5. Experimental similarity densities, $f'(z)$. The solid line represents Eq. (5.1).

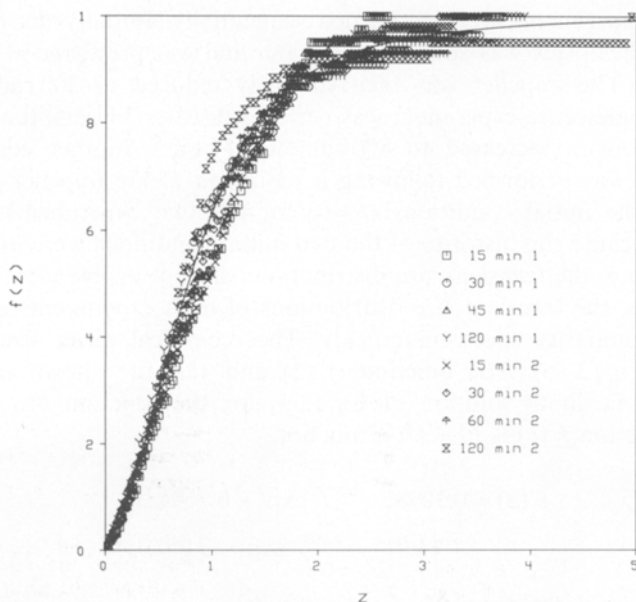


Fig. 6. Experimental cumulative volume fraction $f(z)$ data plotted versus z . The solid line represents Eq. (5.1).

given by Eq. (2.4b). The scaling spectrum given by Eq. (5.1) along with Eq. (2.16) can be used to predict the transient volume fractions and the cumulative volume fractions. The other two parameters required for determining the coagulation frequency (m, a_m) were determined by fitting Eq. (2.16), assuming that m and a_m are the same for both experiments. The only difference between the two experiments is a different integration constant due to the different initial conditions. The parameter m was determined to be 0.44 with a_m equal to $2.48(10^{-4}) \mu l^{1-m} \text{ min}^{-1}$.

Since $(f'(z)/z)(\Psi(z))$ is singular at the origin, $b(z, z')$ is not singular along the axes. Therefore, no estimate of the degree of singularity is needed and the Laguerre polynomials are the basis functions. The fitted spectrum (5.1) is used as the input to the inverse problem scheme [Eq. (2.9)]. The resulting $b(z, z')$ is shown in Fig. 7. Four basis functions are used and thus 10 independent coefficients are determined. This $b(z, z')$ along with the parameters m and a_m determine $q(v, v', \dots)$ completely. The frequency $q(v', v'')$ can now be used to predict transient size distributions by Eq. (1.1).

In order to pick a proper regularization parameter, an estimate of the experimental uncertainty in $F(v, t)$ has to be made. If it is assumed that the actual $f(z)$ is the same for all eight transients, a standard deviation in $F(v, t)$ can be calculated. For these data the standard deviation in $F(v, t)$

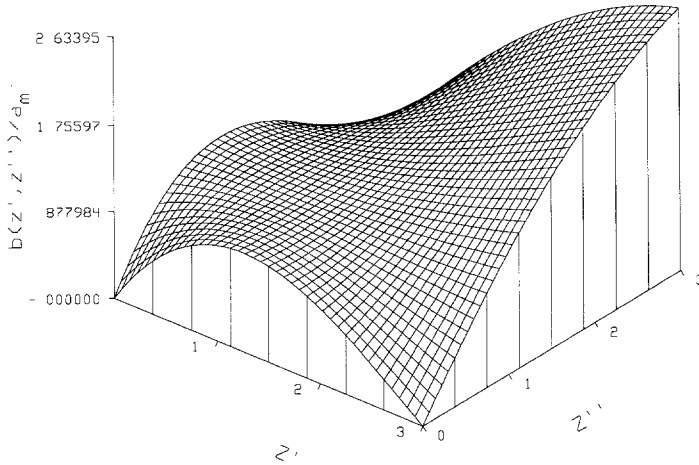


Fig. 7. The unknown function $b(z', z'')/a_m$ determined from the inverse problem for the experimental $f'(z)$.

was 0.035. In accordance with Tikhonov's regularization principle,⁽¹⁴⁾ the regularization parameter was set to be the maximum λ for which the derived coalescence frequency predicts the experimental transients or the similarity-predicted transients to within the estimated uncertainty. The determined regularization parameter is 0.1.

Figures 8 and 9 show the transients predicted by the coalescence frequency along with the similarity-predicted transients from Eqs. (2.16) and (5.1) compared with the experimental data. In both sets of data, the initial condition input to Eq. (1.1) is the number density predicted by Eqs. (5.1) and (2.16) at $t = 15$ min. For both experiments the transients predicted from the similarity distribution, via Eq. (2.3), and the transients predicted by Eq. (1.1) with the obtained frequency match well. The differences between the predictions and the data arise due to two reasons. The first is the inadequacies inherent in the fitting of Eq. (2.16). For example, in experiment 1 the predicted value of $s(t)$ and the experimental value at $t = 45$ min differ by 25% (see Fig. 10). Therefore, the data and predictions show deviations for this time. The second is the experimental deviation of the data from the similarity distribution given by Eq. (5.1). For example, in experiment 2 the 120-min size distribution has the largest deviation from the similarity distribution (see Fig. 6). Thus, the data and predictions differ.

The agglomeration frequency predicted by the inverse problem shows significant deviation from previous models for the frequency. The coalescence frequency for drops in a turbulent flow field has been assumed previously⁽¹⁹⁾ to be of the form of Eq. (4.3), where η_c has frequently been supposed to be a constant. The results from the inverse problem do not

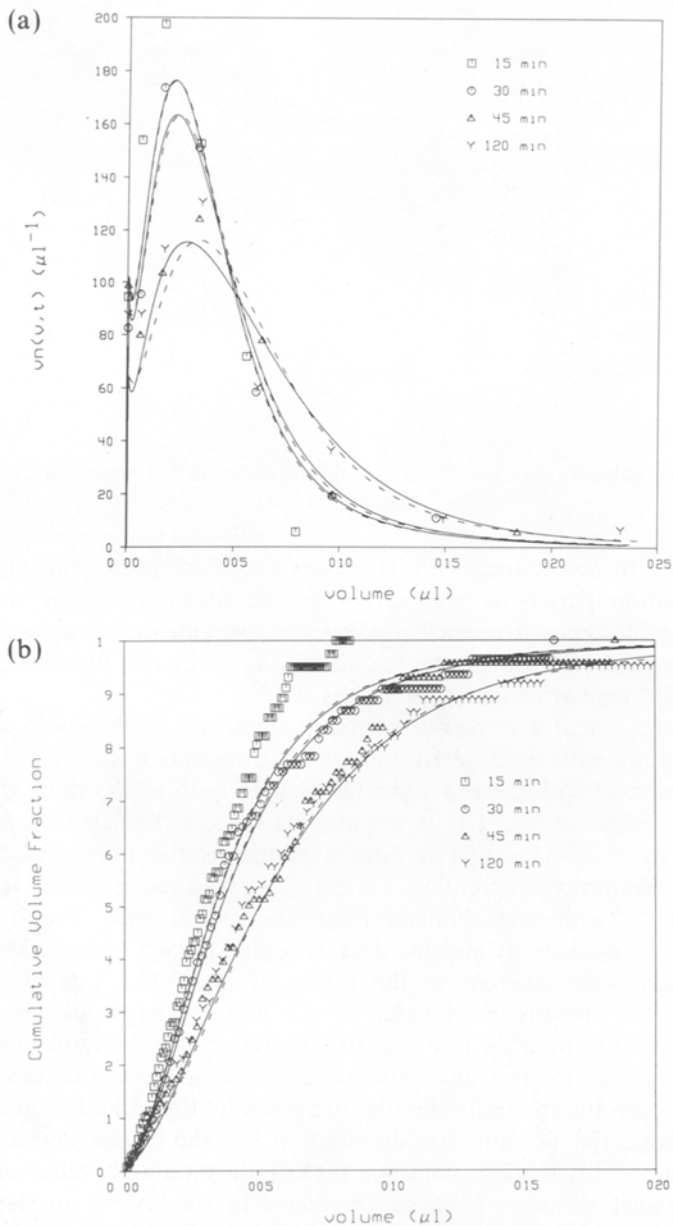


Fig. 8. Transient distributions of experiment 1. The dashed lines represent the predictions from the similarity distribution, Eq. (5.1), making use of the fit of Eq. (2.16). The solid lines represent the predictions of Eq. (1.1). (a) Transient volume fractions $vn(v, t)$ in μl^{-1} . (b) transient cumulative volume fractions $F(v, t)$.

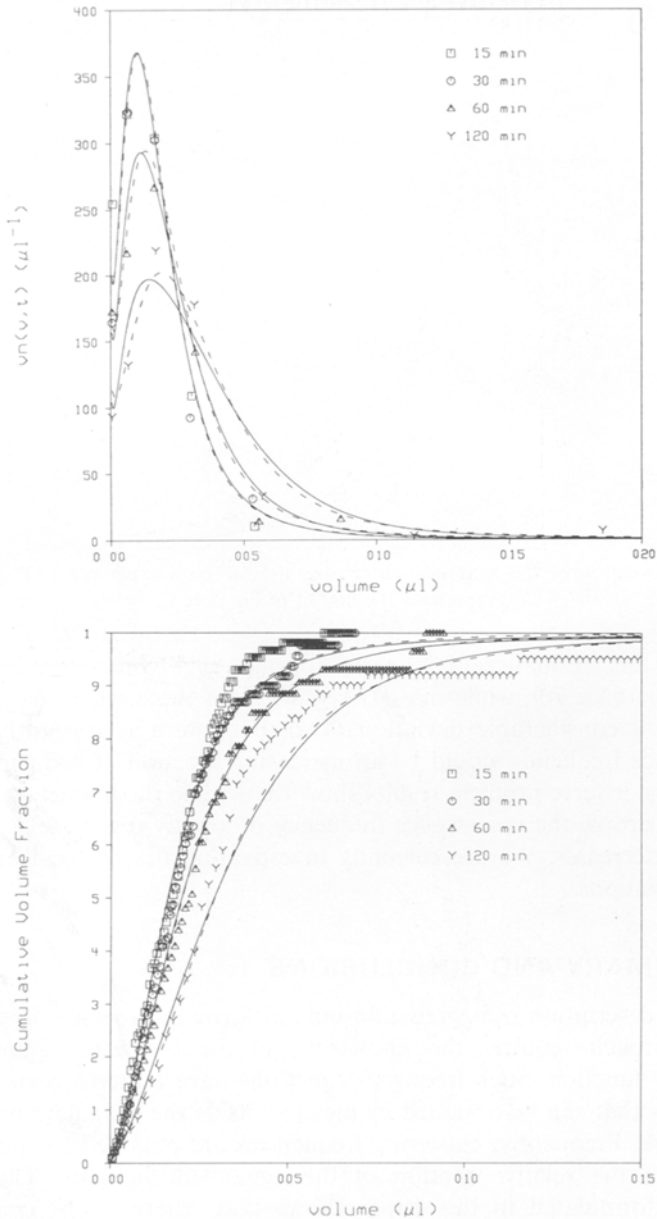


Fig. 9. Transient distributions of experiment 2. The dashed lines represent the predictions from the similarity distribution, Eq. (5.1), making use of the fit of Eq. (2.16). The solid lines represent the predictions of Eq. (1.1). (a) Transient volume fractions $vn(v, t)$ in μl^{-1} . (b) Transient cumulative volume fractions $F(v, t)$.

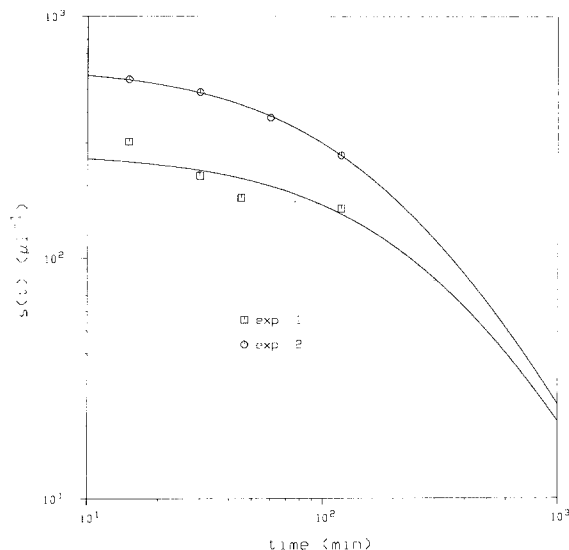


Fig. 10. Evolution of the reciprocal mean size $s(t)$ for both experiments. The solid line represents the best fit of Eq. (2.16).

indicate this. Equation (4.5) with constant η_c would require the m parameter to be $7/9$, while the $s(t)$ evolution for these sets of data predicts $m=0.44$, a considerable deviation. Also, if η_c were a constant, then the coalescence frequency would be an increasing function of drop size for all drops. The inverse problem results show that, while the frequency increases for most drops, the coalescence frequency of greatly disparate-sized drops actually decreases. We are currently investigating the physical origins for these deviations.

6. SUMMARY AND CONCLUSIONS

The description of aggregation-induced growth processes in the mean field approach requires the knowledge of the bivariate agglomeration frequency function. Such frequency functions have hitherto been regarded as entities that can be obtained by means outside the coagulation equation framework. Frequently, clustering frequencies are obtained by mechanistic models of the relative motion of the agglomerating pair. The inverse problem formulated in this paper shows that, alternatively, coagulation frequencies may be extracted from self-similar size spectra in the mean field framework. The inverse problem approach is particularly useful in situations where the dynamics of the collision process is complicated by short-range forces or many-body effects.

An integral equation is derived to extract the coagulation frequency function from dynamic scaling spectra. A suitable basis set for expanding the unknown frequency function can be obtained from the properties of the similarity spectrum itself. The approach is exemplified by subjecting scaling spectra of known agglomeration frequencies to the inverse problem.

The inverse problem is used to extract the agglomeration frequency of droplets in a turbulent flow field from an experimental self-similar distribution. The extracted frequency shows significant deviation from previous models for the agglomeration frequency in a turbulent flow field.

The numerical experiments as well as the test on experimental data show that the inverse problem can be an effective tool for understanding the dynamics of various aggregation processes.

ACKNOWLEDGMENT

The authors gratefully acknowledge the support of the National Science Foundation through grants CBT-8414204 and CBT-8611858.

REFERENCES

1. M. V. Smoluchowski, *Physik. Z.* **17**:557 (1916).
2. S. K. Friedlander, *Smoke, Dust and Haze: Fundamentals of Aerosol Behavior* (Wiley, New York, 1977).
3. M. H. Ernst, in *Fundamental Problems in Statistical Mechanics*, Vol. 6, E. G. D. Cohen, ed. (North-Holland, Amsterdam, 1985).
4. J. Feder, T. Jossang, and E. Rosenqvist, *Phys. Rev. Lett.* **53**:1403 (1984).
5. F. Family and D. P. Landau, in *Kinetics of Aggregation and Gelation*, F. Family and D. P. Landau, eds. (North-Holland, Amsterdam, 1986).
6. F. Family and T. Vicsek, in *Physics of Finely Divided Matter*, N. Boccara and M. Daoud, eds. (Springer-Verlag, Berlin, 1985).
7. R. M. Ziff, M. H. Ernst, and E. M. Hendriks, *J. Phys. A: Math. Gen.* **16**:2293 (1983).
8. D. L. Swift and S. K. Friedlander, *J. Colloid Interface Sci.* **19**:621 (1964).
9. R. Muralidhar and D. Ramkrishna, *J. Colloid Interface Sci.* **112**:348 (1986).
10. R. Muralidhar and D. Ramkrishna, *J. Colloid Interface Sci.* **131**:503 (1989).
11. P. G. J. van Dongen and M. H. Ernst, *J. Stat. Phys.* **50**:295 (1988).
12. C. S. Wang, Ph. D. Thesis, California Institute of Technology (1966).
13. C. S. Wang and S. K. Friedlander, *J. Colloid Interface Sci.* **24**:170 (1967).
14. L. M. Delves and J. L. Mohamed, *Computational Methods for Integral Equations* (Cambridge University Press, London, 1987).
15. D. Ramkrishna, *Chem. Eng. Sci.* **28**:1362 (1973).
16. R. Courant and D. Hilbert, *Methods of Mathematical Physics*, Vol. 1 (Wiley, New York, 1962).
17. R. Muralidhar and D. Ramkrishna, *Ind. Eng. Chem. Fund.* **25**:554 (1986).
18. T. G. Tobin, R. Muralidhar, H. Wright, and D. Ramkrishna, *Chem. Eng. Sci.* (in press).
19. V. G. Levich, *Physicochemical Hydrodynamics* (Prentice-Hall, New York, 1962).